特戊酸和含氮配体构筑的 Ln(Ⅲ)配合物的结构、热稳定性和荧光性质

方洁芳　熊艳菊　程靖祥　黄树婷　方乐欣　陆　珣　乐善堂*
(华南师范大学化学与环境学院,广州　510006)

摘要：在水热条件下 2 个配体特戊酸 (pivH) 和 1-*H*-咪唑 [4,5-*f*][1,10]-菲咯啉(IP)和稀土金属反应得到了 6 个稀土配合物 [Ln(piv)₃(IP)₂], (Ln=Nd(**1**), Eu(**2**), Gd(**3**), Tb(**4**), Dy(**5**), Ho(**6**))。结果显示,2 个混合配体和不同的稀土金属形成了 6 个相似的零维结构,进而通过 N-H···O 氢键和 π-π 堆积作用,形成一维链状结构。6 个配合物均用元素分析、粉末衍射(PXRD)、红外光谱(FTIR)进行了表征,且对配合物 **2** 和 **4** 的荧光性质及 **1** 和 **2** 的热稳定性进行了详细的分析。

关键词：稀土配合物；特戊酸；荧光性质；热重分析

Lanthanide(Ⅲ) Coordiantion Complexes with Pivalates and Chelating N-Donor Ligands: Syntheses, Structures, Thermal Stabilities and Luminescence Properties

FANG Jie-Fang　XIONG Yan-Ju　CHENG Jing-Xiang　HUANG Shu-Ting
FANG Le-Xin　LU Xun　YUE Shan-Tang*
(*School of Chemistry and Environment, South China Normal University, Guangzhou* 510006, *China*)

Abstract: A series of novel monometallic coordination complexes [Ln(piv)₃(IP)₂], (Ln=Nd (**1**), Eu(**2**), Gd(**3**), Tb (**4**), Dy(**5**), Ho(**6**), IP=1-*H*-imidazo[4,5-*f*][1,10]-phenanthroline, pivH=pivalic acid) have been successfully synthesized under hydrothermal condition. Complexes **1~6** have been determined by single-crystal X-ray diffraction analyses, elemental analyses, IR spectroscopy and powder X-ray diffraction. The result reveals that all the six new complexes present similar 0-dimensional structures, which are further extended into the one-dimensional (1D) architectures through hydrogen bonds and π-π stacking interactions. Meanwhile, the thermogravimetric analyses of complexes **1** and **2** and photoluminescent properties of complexes **2** and **4** have also been investigated. CCDC: 1476957, **1**; 1476958, **2**; 1476959, **3**; 1476960, **4**; 1476961, **5**; 1476962, **6**.

Keywords: Ln(Ⅲ) complex; pivalic acid; luminescent; thermogravimetric analysis

0　Introduction

　　The versatile lanthanide complexes with novel structures and optical properties have recently drawn considerable focus as a result of their promising applications in many fields[1-3]. Especially, lanthanide (Ⅲ) coordination polymers have unique properties such as line-like emission, high color purity, long luminescence lifetime and high quantum yields [4]. However, in general, the spin/parity- forbidden nature of the *f-f* transitions of lanthanide (Ⅲ) ion results in abominably low molar extinction coefficients and weak

luminescence intensity[5-8]. Nevertheless, this drawback can be overcome when organic ligands acting as the sensitizer are introduced into the systems. As a result, chromophoric antenna ligands, specially, π-conjugated organic chromophores have been of intense interest owning to their broad and intense adsorption band in ultraviolet[5]. So conjugated and rigid multidentate 1-H-imidazo[4,5-f][1,10]-phenanthroline (IP) is chosen as a ligand. Whats more, if the coordination sites of the lanthanide ions can be filled up, the radiationless deactivation processes maybe diminish[9]. In this aspect, pivalic acid (pivH), as a sterically hindered carboxylate ligand[10], together with lanthanide(Ⅲ) ions are applied to prepare low-dimensional structures.

By this strategy, six new monometallic Ln (Ⅲ) complexes, ([Ln(piv)$_3$(IP)$_2$], (Ln=Nd (**1**), Eu (**2**), Gd (**3**), Tb (**4**), Dy (**5**), Ho (**6**)) were obtained under hydrothermal condition. Block crystals of complexes **1~6** were synthesized with a mixture of pivH, IP and Ln$_2$O$_3$ in a 1:1:1 molar ratio in 10 mL water at 433 K for 3 days. Only when Lanthanide oxides were employed can the crystals be obtained. If the lanthanide nitrates were used under the various conditions, such as temperature, reaction time, pH value and solvent, none of targeted products can be afforded.

1 Experimental

1.1 Materials and methods

All chemicals employed were commercially available and used as received without further purificaion. Elemental (C, H, N) analyses were performed on a Perkin-Elmer 2400 element analyzer. The FTIR spectra were recorded from KBr pellets in the range of 4 000~400 cm^{-1} on a Nicolet 6700 spectrometer. Thermogravimetric analyses were performed on Perkin-Elmer TGA 7 analyzer with a heating rate of 10 ℃·min^{-1} in flowing air atmosphere. Luminescence spectroscopy was recorded on an Edinburgh F900 FLS-900 spectrophotometer analyzer with a xenon arc lamp as the light source. In the measurement of emission and excitation spectra, the pass width is 5.0 nm. Powder X-ray diffraction (PXRD) patterns were recorded on a X-pert diffractometer or Rigaku D/M-2200T automated

diffractometer for Cu $K\alpha$ radiation (λ=0.154 056 nm), with operating voltage of 40 kV, current of 15 mA, a scan speed of 4°·min^{-1} and a step size of 0.02° in 2θ range of 5°~50°.

1.2 Syntheses of complexes 1~6

A mixture of pivH (0.166 1 g, 0.5 mmol), IP (0.127 g, 0.5 mmol), Nd$_2$O$_3$ for **1** (0.168 2 g, 0.5 mmol), Eu$_2$O$_3$ for **2** (0.176 0 g, 0.5 mmol), Gd$_2$O$_3$ for **3** (0.181 2 g, 0.5 mmol), Tb$_4$O$_7$ for **4** (0.186 9 g, 0.25 mmol), Dy$_2$O$_3$ for **5** (0.118 65 g, 0.5 mmol), Ho$_2$O$_3$ for **6** (0.188 9 g, 0.5 mmol) and H$_2$O(10 mL) was sealed in a 23 mL Teflon-lined stainless-steel autoclave, then heated to 160 ℃ for 72 h. After cooling to room temperature at a rate of 3 ℃·h^{-1}, colorless block crystals(complex **1** is purple) were collected manually, washed with distilled water for several times and dried in air. For **1**, 55% yield based on Nd. Anal. Calcd. for C$_{41}$H$_{43}$NdN$_8$O$_6$ (%): C, 55.40; H, 4.84; N, 12.61. Found (%): C, 55.40; H, 4.85; N, 12.60. For **2**, 78% yield based on Eu. Anal. Calcd. for C$_{41}$H$_{43}$EuN$_8$O$_6$ (%): C, 54.92; H, 4.80; N, 12.50%. Found (%): C, 54.95; H, 4.77; N, 12.50%. For **3**, 73% yield based on Gd. Anal. Calcd. for C$_{41}$H$_{43}$GdN$_8$O$_6$ (%): C, 54.60; H, 4.77; N, 12.43. Found(%): C, 54.68; H, 4.75; N, 12.37. For **4**, 71% yield based on Tb. Anal. Calcd. for C$_{41}$H$_{43}$TbN$_8$O$_6$ (%): C, 55.50; H, 4.76; N, 12.41. Found (%): C, 55.53; H, 4.74; N, 12.40. For **5**, 77% yield based on Dy. Anal. Calcd. for C$_{41}$H$_{43}$DyN$_8$O$_6$(%): C, 54.28; H, 4.74; N, 12.36. Found(%): C, 54.29; H, 4.75; N, 12.34. For **6**, 66% yield based on Ho. Anal. Calcd. for C$_{41}$H$_{43}$HoN$_8$O$_6$ (%): C, 54.14; H, 4.73; N, 12.32. Found(%): C, 54.15; H, 4.71; N, 12.33.

1.3 X-ray data collection and structure refinement

Data collections were performed at 296 K on a Bruker Apex Ⅱ Smart CCD diffractometer with graphite-monochromated Mo $K\alpha$ radiation(λ=0.071 073 nm) for complexes **1~6**. Multi-scan absorption corrections were applied by using the program SADABS[11]. Structural solutions and full-matrix least-squares refinements based on F^2 were performed with the SHELXL-97 and SHELXS-97[12] program packages, respectively. Anisotropic thermal parameters were used to refine all non-H atoms. The hydrogen atoms

for C-H and N-H were placed in idealized positions. Details of the crystal parameters, data collections, and refinements for complexes **1 ~6** are summarized in Table 1. Selected bond lengths and angles are listed in Table 2. Hydrogen bond lengths and angles for complex **4** are listed in Table 3.

CCDC:1476957, **1**; 1476958, **2**; 1476959, **3**;

1476960, **4**; 1476961, **5**; 1476962, **6**.

2　Results and discussion

2.1　Description of the structures of complexes 1~6

To the best of our knowledge, the lanthanide supramolecular complexes based on both piv⁻ and IP ligands have never been reported. The IR spectra of

Table 1　Crystallographic and structural refinement parameters for complexes 1~6

Complex	1	2	3	4	5	6
Formula	$C_{41}H_{43}NdN_8O_6$	$C_{41}H_{43}EuN_8O_6$	$C_{41}H_{43}GdN_8O_6$	$C_{41}H_{43}TbN_8O_6$	$C_{41}H_{43}DyN_8O_6$	$C_{41}H_{43}HoN_8O_6$
Molecular weight	888.07	895.8	901.08	902.76	906.33	908.76
Crystalsystem	Monoclinic	Monoclinic	Monoclinic	Monoclinic	Monoclinic	Monoclinic
Space group	Cc	Cc	Cc	$P2_1/c$	$P2_1/c$	$P2_1/c$
a / nm	1.326 6(7)	1.328 1 6(11)	1.333 0(4)	1.335 12(19)	1.343 19(17)	1.346 25(14)
b / nm	1.525 8(7)	1.510 7 8(12)	1.511 0(5)	1.501 9(2)	1.503 38(19)	1.504 99(16)
c / nm	2.125 4(10)	2.109 3 7(18)	2.112 7(7)	2.109 8(3)	2.112 6(3)	2.112 8(2)
β / (°)	102.604(5)	102.838 0(10)	102.836(4)	103.201(2)	103.836(2)	104.134 0(10)
V / nm³	4.198(4)	4.126 8(6)	4.149(2)	4.118 8(10)	4.142 2(9)	4.151 1(8)
Z	4	4	4	4	4	4
D_c / (g·cm⁻³)	1.405	1.442	1.443	1.456	1.453	1.454
μ / mm⁻¹	1.291	1.575	1.653	1.772	1.859	1.961
$F(000)$	1 812	1 824	1 828	1 832	1 836	1 840
Reflections collected, unique	19 443, 7 559	10 279, 5 091	7 876, 5 123	16 190, 7 247	20 619, 7 286	19 845, 6 944
Observed reflection ($I>2\sigma(I)$)	3 530	3 993	2 999	3 753	4 675	4 559
R_{int}	0.128 9	0.037 0	0.076 4	0.050 9	0.058 0	0.054 6
GOF	1.030	1.092	1.053	0.868	1.169	0.901
R_1^a, wR_2^b	0.087 0,0.196 3	0.053 8, 0.145 5	0.070 8, 0.160 4	0.044 9, 0.094 9	0.043 5, 0.178 9	0.043 5, 0.112 9
R_1^a, wR_2^b	0.180 5,0.252 9	0.073 2, 0.165 8	0.117 1, 0.191 6	0.080 5, 0.107 0	0.102 7, 0.206 8	0.078 4, 0.141 3

^{a} $R_1 = \sum ||F_o| - |F_c|| / \sum |F_o|$; ^{b} $wR_2 = \{\sum [w(F_o^2 - F_c^2)^2]/ \sum (F_o^2)^2\}^{1/2}$

Table 2　Selected bond lengths (nm) and angles (°) for complexes 1~6

Complex **1**					
Nd(1)-O(3)	0.254(2)	Nd(1)-O(2)	0.252 5(15)	Nd(1)-N(2)	0.260(2)
Nd(1)-O(6)	0.258(2)	Nd(1)-O(5)	0.268(2)	Nd(1)-N(6)	0.272 7(16)
Nd(1)-O(4)	0.252(2)	Nd(1)-N(1)	0.257(2)	Nd(1)-N(5)	0.281(2)
Nd(1)-O(1)	0.254 2(18)				
O(6)-Nd(1)-O(4)	72.7(8)	O(4)-Nd(1)-O(5)	84.8(8)	O(2)-Nd(1)-N(5)	113.8(7)
O(3)-Nd(1)-O(1)	82.4(7)	N(1)-Nd(1)-N(2)	64.0(6)	O(5)-Nd(1)-N(5)	115.5(6)
O(6)-Nd(1)-O(1)	126.3(7)	N(1)-Nd(1)-N(6)	90.4(6)	O(6)-Nd(1)-N(6)	112.4(5)
O(4)-Nd(1)-O(1)	71.4(7)	N(2)-Nd(1)-N(6)	66.9(3)	O(4)-Nd(1)-N(6)	131.3(7)
O(3)-Nd(1)-O(2)	71.7(7)	N(1)-Nd(1)-N(5)	142.6(4)	O(1)-Nd(1)-N(6)	67.8(6)

Continued Table 2

O(6)-Nd(1)-O(2)	174.1(7)	N(2)-Nd(1)-N(5)	82.1(7)	O(2)-Nd(1)-N(6)	70.0(6)
O(4)-Nd(1)-O(2)	101.5(7)	N(6)-Nd(1)-N(5)	60.5(6)	O(5)-Nd(1)-N(6)	138.0(6)
O(1)-Nd(1)-O(2)	48.9(6)	O(6)-Nd(1)-N(2)	69.5(7)	O(3)-Nd(1)-N(5)	133.6(7)

Complex 2

Eu(1)-O(1)	0.246(3)	Eu(1)-O(2)	0.258 5(19)	N(7)-Eu(1)	0.257 3(8)
Eu(1)-O(3)	0.247(2)	Eu(1)-O(6)	0.258 9(18)	N(4)-Eu(1)	0.263 7(8)
Eu(1)-O(4)	0.248 3(15)	N(8)-Eu(1)	0.266 1(9)	N(3)-Eu(1)	0.258 9(11)
Eu(1)-O(5)	0.252 2(18)				
O(3)-Eu(1)-O(4)	52.2(5)	N(7)-Eu(1)-N(3)	87.1(2)	O(5)-Eu(1)-N(3)	113.0(5)
O(1)-Eu(1)-O(5)	174.2(5)	N(7)-Eu(1)-N(8)	62.54(17)	O(6)-Eu(1)-N(4)	67.9(5)
O(3)-Eu(1)-O(5)	103.5(6)	N(3)-Eu(1)-N(4)	62.79(19)	N(7)-Eu(1)-O(2)	71.3(4)
O(4)-Eu(1)-O(5)	72.3(6)	O(4)-Eu(1)-N(7)	134.5(5)	O(3)-Eu(1)-N(4)	135.8(5)
O(1)-Eu(1)-O(2)	50.6(7)	O(5)-Eu(1)-N(7)	113.7(5)	O(4)-Eu(1)-N(4)	140.8(5)
O(3)-Eu(1)-O(2)	82.3(6)	O(1)-Eu(1)-N(3)	70.1(6)	O(5)-Eu(1)-N(4)	68.6(5)
O(4)-Eu(1)-O(2)	70.5(6)	O(3)-Eu(1)-N(3)	83.6(6)	N(7)-Eu(1)-N(4)	67.55(19)
O(5)-Eu(1)-O(2)	126.4(7)	O(4)-Eu(1)-N(3)	134.1(5)	O(2)-Eu(1)-N(4)	138.5(4)

Complex 3

Gd(1)-O(4)	0.240(2)	Gd(1)-O(2)	0.254 4(16)	Gd(1)-N(8)	0.259(3)
Gd(1)-O(1)	0.251 0(17)	Gd(1)-O(6)	0.270 9(18)	Gd(1)-N(3)	0.264(3)
Gd(1)-O(5)	0.251(2)	Gd(1)-N(4)	0.255 7(16)	Gd(1)-N(7)	0.272 4(19)
Gd(1)-O(3)	0.2527(17)				
O(4)-Gd(1)-O(3)	51.4(4)	N(8)-Gd(1)-N(7)	58.5(8)	O(5)-Gd(1)-O(6)	54.2(6)
O(1)-Gd(1)-O(3)	100.8(5)	N(4)-Gd(1)-N(7)	67.0(3)	O(3)-Gd(1)-O(6)	92.0(6)
O(5)-Gd(1)-O(3)	70.5(6)	N(8)-Gd(1)-N(3)	142.8(4)	O(2)-Gd(1)-O(6)	153.5(4)
O(4)-Gd(1)-O(2)	75.8(6)	O(5)-Gd(1)-N(4)	72.2(6)	N(4)-Gd(1)-O(6)	65.8(5)
O(1)-Gd(1)-O(2)	49.2(5)	O(3)-Gd(1)-N(4)	142.6(5)	N(8)-Gd(1)-O(6)	118.7(7)
O(5)-Gd(1)-O(2)	123.2(6)	O(2)-Gd(1)-N(4)	140.7(5)	N(3)-Gd(1)-O(6)	66.6(7)
O(3)-Gd(1)-O(2)	65.2(5)	O(4)-Gd(1)-N(8)	131.8(8)	O(4)-Gd(1)-N(7)	141.7(6)
N(4)-Gd(1)-N(8)	83.1(7)	O(1)-Gd(1)-N(8)	111.3(7)	O(1)-Gd(1)-N(7)	70.5(5)
N(4)-Gd(1)-N(3)	65.2(7)	O(5)-Gd(1)-N(8)	66.6(8)	O(5)-Gd(1)-N(7)	113.5(6)

Complex 4

Tb(1)-O(6)	0.242 1(5)	Tb(1)-O(4)	0.259 (5)	Tb(1)-N(5)	0.257 6(4)
Tb(1)-O(3)	0.244 5(5)	Tb(1)-O(1)	0.273 7(7)	Tb(1)-N(8)	0.259 5(5)
Tb(1)-O(2)	0.244 5(6)	Tb(1)-N(6)	0.256 3(5)	Tb(1)-N(7)	0.261 7(5)
Tb(1)-O(5)	0.246 0(4)				
O(6)-Tb(1)-O(3)	98.65(19)	N(6)-Tb(1)-N(8)	143.73(15)	N(6)-Tb(1)-O(4)	69.70(16)
O(6)-Tb(1)-O(2)	72.6(2)	N(5)-Tb(1)-N(8)	86.50(16)	N(5)-Tb(1)-O(4)	68.03(15)
O(3)-Tb(1)-O(2)	169.7(2)	N(6)-Tb(1)-N(7)	86.22(16)	N(8)-Tb(1)-O(4)	119.13(16)
O(6)-Tb(1)-O(5)	52.09(18)	N(5)-Tb(1)-N(7)	67.59(14)	O(6)-Tb(1)-N(7)	142.75(19)
O(3)-Tb(1)-O(5)	73.61(18)	N(8)-Tb(1)-N(7)	62.65(16)	O(3)-Tb(1)-N(7)	118.39(17)
O(2)-Tb(1)-O(5)	96.4(2)	O(6)-Tb(1)-N(6)	81.00(17)	O(2)-Tb(1)-N(7)	70.13(18)
O(6)-Tb(1)-O(1)	87.62(18)	O(3)-Tb(1)-N(6)	115.42(16)	O(5)-Tb(1)-N(7)	132.35(17)
O(3)-Tb(1)-O(1)	127.64(19)	O(2)-Tb(1)-N(6)	69.3(2)	O(4)-Tb(1)-N(7)	135.33(15)

Continued Table 2

		Complex 5			
Dy(1)-O(6)	0.234 1(7)	Dy(1)-O(3)	0.245 0(5)	Dy(1)-N(6)	0.255 7(5)
Dy(1)-O(1)	0.240 1(5)	Dy(1)-N(5)	0.251 7(6)	Dy(1)-N(1)	0.256 8(6)
Dy(1)-O(4)	0.241 0(5)	Dy(1)-O(2)	0.264 6(6)	Dy(1)-N(2)	0.259 9(6)
O(6)-Dy(1)-O(1)	162.7(3)	N(6)-Dy(1)-N(2)	67.74(18)	O(4)-Dy(1)-N(1)	135.38(18)
O(6)-Dy(1)-O(4)	74.2(2)	N(1)-Dy(1)-N(2)	62.97(18)	O(3)-Dy(1)-N(1)	82.50(18)
O(1)-Dy(1)-O(4)	93.9(2)	N(5)-Dy(1)-N(6)	64.42(18)	O(6)-Dy(1)-N(2)	70.6(2)
O(6)-Dy(1)-O(3)	87.0(3)	N(5)-Dy(1)-N(1)	143.66(19)	O(1)-Dy(1)-N(2)	121.6(2)
O(1)-Dy(1)-O(3)	75.7(2)	N(6)-Dy(1)-N(1)	86.88(18)	O(4)-Dy(1)-N(2)	144.4(2)
O(4)-Dy(1)-O(3)	52.89(19)	N(5)-Dy(1)-N(2)	84.78(18)	O(3)-Dy(1)-N(2)	128.83(19)
O(6)-Dy(1)-O(2)	132.0(2)	O(6)-Dy(1)-N(5)	73.9(3)	O(4)-Dy(1)-N(6)	131.11(18)
O(1)-Dy(1)-O(2)	50.38(19)	O(1)-Dy(1)-N(5)	117.16(18)	O(3)-Dy(1)-N(6)	150.54(19)
		Complex 6			
Ho(1)-O(5)	0.231 2(7)	Ho(1)-O(3)	0.265 9(6)	Ho(1)-N(7)	0.253 1(5)
Ho(1)-O(4)	0.237 7(6)	Ho(1)-O(1)	0.243 1(5)	Ho(1)-N(4)	0.254 0(5)
Ho(1)-O(2)	0.238 8(5)	Ho(1)-N(3)	0.251 1(6)	Ho(1)-N(8)	0.258 8(6)
O(5)-Ho(1)-O(4)	159.1(3)	O(1)-Ho(1)-O(3)	97.95(19)	O(1)-Ho(1)-N(4)	151.89(19)
O(5)-Ho(1)-O(2)	74.5(2)	N(3)-Ho(1)-N(7)	143.70(18)	O(5)-Ho(1)-N(8)	70.6(2)
O(4)-Ho(1)-O(2)	92.2(2)	N(7)-Ho(1)-N(4)	87.17(17)	O(4)-Ho(1)-N(8)	123.45(19)
O(5)-Ho(1)-O(1)	83.0(2)	N(3)-Ho(1)-N(8)	84.05(18)	O(2)-Ho(1)-N(8)	144.26(19)
O(4)-Ho(1)-O(1)	76.2(2)	N(7)-Ho(1)-N(8)	63.29(17)	O(1)-Ho(1)-N(8)	127.22(18)
O(2)-Ho(1)-O(1)	53.75(18)	N(4)-Ho(1)-N(8)	68.01(18)	N(3)-Ho(1)-O(3)	69.91(18)
O(5)-Ho(1)-O(3)	133.7(2)	O(5)-Ho(1)-N(3)	76.2(3)	N(7)-Ho(1)-O(3)	121.07(17)
O(4)-Ho(1)-O(3)	50.46(18)	O(4)-Ho(1)-N(3)	118.02(19)	O(1)-Ho(1)-N(3)	133.40(18)

Table 3　Hydrogen bonding data for complex 4

D-H⋯A	d(D-H) / nm	d(H⋯A) / nm	d(D⋯A) / nm	∠DHA / (°)
N(1)-H(1)⋯O(4)	0.086	0.192	0.275 1(7)	163
N(4)-H(4)⋯O(1)	0.086	0.193	0.276 6(9)	163

all complexes exhibit similarities (Suppourting information). The absorption peaks around 3 450 cm⁻¹ was assigned to the N-H stretching vibrations. There are strong absorption peaks around 1 618~1 561 cm⁻¹ (antisymmetric stretching vibrations) and 1 399~1 376 cm⁻¹ (symmetric stretching vibrations). Closer inspection shows that there are no absorption peaks around 1 700 cm⁻¹ indicating that carboxyl groups are of completely deprotonation[13].

X-ray single-crystal diffraction reveals that complexes **1**~**6** crystallize in the monoclinic system with similar cell parameters. All complexes present the same molecular structures although the coordination number is a little different. Complexes **1**~**4** are ten-coordinated while **5**~**6** are nine-coordinated. It may be assigned to the lanthanide contraction effect[14-15]. Herein only the structure of **4** is described in detail. The asymmetric unit of complex **4** consists of one crystallographically independent Tb(Ⅲ) ion, three completely deprotonated piv⁻ ligands, two IP ligands. As shown in Fig.1a, the center Tb(Ⅲ) is ten-coordinated by six oxygen atoms from three piv⁻ ligands, four nitrogen atoms from two IP ligands, forming a somewhat distorted two-capped quadrangular

prism coordination geometry. The bond lengths of Tb-O span the range of 0.242 1 (5)~0.273 7 (7) nm and the bond lengths of Tb-N are in the range of 0.256 3(5) ~0.261 7(5) nm. In addition, in the structure of **4**, the N-Tb-N bond angle are in the range of 62.65 (17)°~ 143.73(16)°, and the bond angle of O-Tb-O and O-Tb-N are in the range of 48.2(2)°~169.7(2)° and 67.36(16)° ~157.19(18)°, respectively. Closer inspection shows that there are two types of hydrogen bonds between phenanthroline nitrogens atom and carboxylic oxygen atoms (N1-H⋯O4 0.275 3(7) nm, N4-H⋯O1 0.276 6(9) nm). The mononuclear molecules are linked by these hydrogen bonds in -AA- mode to afford a 1D boundless chain(Fig.1b). In addition, the π-π stacking interactions also exist between the two neighboring IP ligands with the average center to-center distance of *ca.* 0.357 9 nm, which further consolidate the structure.
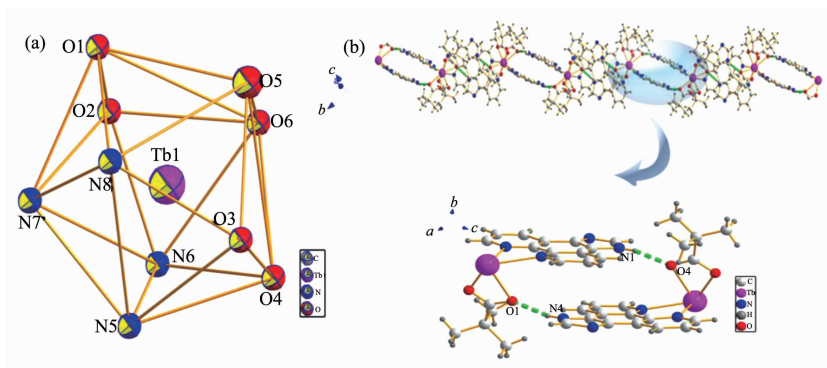

Fig.1 Structure of complex **4**: (a) Coordination polyhedron geometry of the Tb(Ⅲ) ion; (b)1D structure connected by hydrogen bonds

2.2 PXRD results and thermal analyses

Powder X-ray diffraction (PXRD) experiments were performed on complexes **1~6** at room temperature to estimate if the crystalline samples are of phase purity. All major peaks in the measured patterns match quite well with those of the simulated ones, indicating that the bulk as-prepared products are pure (Fig.2).

The isomorphous structures result in a similar thermal decomposition process, so complexes **1** and **2** were chosen as representative examples for thermogravimetric analyses in order to estimate the stability of the complexes. TGA experiments were carried out on these new crystalline materials in the temperature range of 30~750 ℃ with a heating rate of 10 ℃·min⁻¹ in dry air atmosphere, as illustrated in Fig.3. Complex **1** shows no obvious weight loss process under 355 ℃ (358 ℃ for **2**), exhibiting a high thermal stability as there are no coordinated water molecules or solvent molecules in the coordination structure. With the temperature increasing, complexes began to experience stepwise destructive changes, which are ascribed to decomposition of the organic
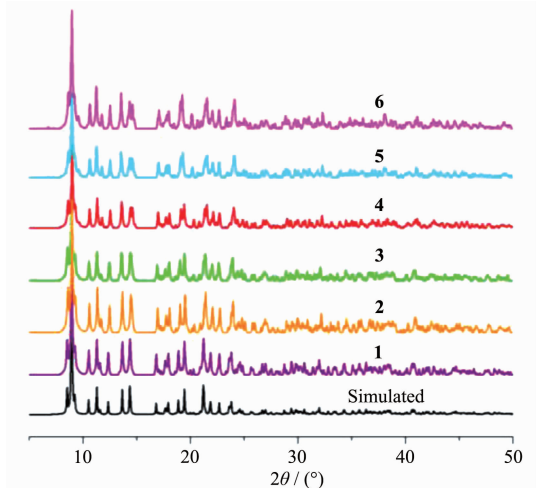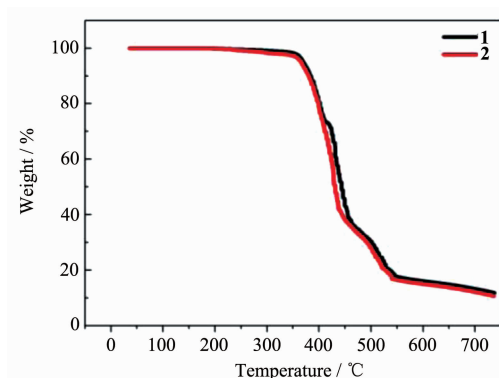

Fig.2 Powder X-ray diffraction patterns of complexes **1~6**

Fig.3 TGA curves for complexes **1~2**

ligands and result in the collapse of whole structure.

2.3 Photoluminescent properties

As shown in Fig.4, the solid-state luminescent properties of complexes of **2** and **4** were investigated in the range of 400~750 nm at ambient temperature. The Eu-based complex of **2** emits intense red fluorescence upon excitation at 350 nm, exhibiting characteristic bands at 579 ($^5D_0{\rightarrow}^7F_0$), 593 ($^5D_0{\rightarrow}^7F_1$), 618 ($^5D_0{\rightarrow}^7F_2$), 652 ($^5D_0{\rightarrow}^7F_3$) and 694 nm($^5D_0{\rightarrow}^7F_4$). The $^5D_0{\rightarrow}^7F_0$ and $^5D_0{\rightarrow}^7F_3$ transition are relative weak, which are regarded as both strictly forbidden in magnetic-dipole (MD) and electric dipole (ED) schemes[5,14-18]. It can be noted that $^5D_0{\rightarrow}^7F_1$ and $^5D_0{\rightarrow}^7F_2$ are the more intense transitions. The $^5D_0{\rightarrow}^7F_1$ is a MD-allowed transition and insensitive to the local environment around Eu(Ⅲ) ions. However, the $^5D_0{\rightarrow}^7F_2$ transition is an ED transition, of which the intensity decreases as the site symmetry of Eu(Ⅲ) increases[13-14]. The luminescent intensity ratio of $I_{^5D_0{\rightarrow}^7F_2}/I_{^5D_0{\rightarrow}^7F_1}$ is approximate 1.3, which suggests that Eu(Ⅲ) ions in **2** have a relatively high centrosymmetric coordination environment matching well with the results of the single-crystal X-ray analysis. On complexation of IP and piv⁻ with Tb(Ⅲ), complex **4** generates pure green luminescence. The emission peaks occur at 490, 545, 585 and 622 nm when excited at 394 nm, corresponding to $^5D_4{\rightarrow}^7F_6$, $^5D_4{\rightarrow}^7F_5$, $^5D_4{\rightarrow}^7F_4$, $^5D_4{\rightarrow}^7F_3$, respectively.
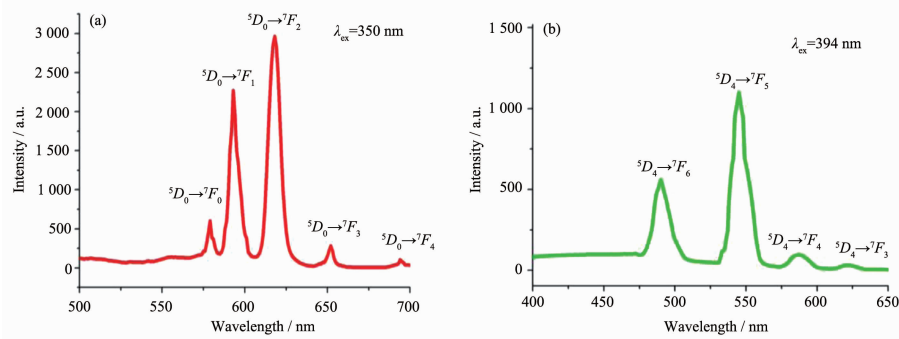

Fig.4　Solid state emissions spectra of complexes **2** and **4** at ambient temperature

3 Conclusions

In summary, six Ln(Ⅲ)-monometallic-based coordination complexes have been successfully prepared by using Ln_2O_3 and mixed ligands IP and piv⁻. Ligand piv⁻ plays a sterically hindered role and may offers a suitable acidic environments to construct the complexes. Thermogravimetric analyses reveal that complexes exhibit high thermal stability. Furthermore, complexes **2** and **4** exhibit excellent characteristic lanthanide-centered luminescent properties.

Supporting information is available at http://www.wjhxxb.cn

References:

[1] An J, Geib S J, Rosi N L. *J. Am.Chem. Soc.*, **2009**,**131**(24): 8376-8377

[2] Dohner E R, Hoke E T, Karunadasa H I. *J. Am. Chem. Soc.*, **2014**,**136**(5):1718-1721

[3] Struzhkin V V, Militzer B , Mao W L, et al. *Chem. Rev.*, **2007**,**131**(10):4133-4151

[4] Shi W J, Hou L, Zhao W, et al. *Inorg. Chem. Commun.*, **2011**, **14**(12):1915-1919

[5] Zhang S, Yang Y, Xia Z Q, et al. *Inorg. Chem.*, **2014**,**53**(20): 10952-10963

[6] Feng X, Feng Y Q, Liu L. *Dalton Trans.*, **2013**,**42**(21):7741 -7754

[7] ZHANG Qing (张青),LIU Chu-Bo(刘春波).CHE Guang-Bo (车广波), et al. *Chinese J. Inorg. Chem.*(无机化学学报), **2013**,**29**(10):2188-2194

[8] RAN Xing-Rui(冉行蕊), XIE Wei-Ping(谢卫萍), XIONG Yan-Ju(熊艳菊), et al. *Chinese J. Inorg. Chem.*(无机化学学报), **2014**,**30**(11):2662-2668

[9] Fomina I G, Dobrokhotova Z V, Kazak V O, et al. *Eur. J. Inorg. Chem.*, **2012**,**2012**(22):3595-3610

[10]Liu S J, Zhao J P, Song W C, et al. *Inorg. Chem.*, **2013**,**52** (4):2103-2109

[11]Sheldrick G M. *SADABS*, University of Göttingen, Germany, **1996**.

[12](a) Sheldrick G M. *SHELXL*-97, *Program for X-ray Structure Determination*, University of Göttingen, Göttingen,

　　　Germany, **1997**.

　(b) Sheldrick G M. *SHELXS*-97, *Program for X-ray Crystal Structure Refinement*, University of Göttingen, Göttingen, Germany, **1997**.

[13]Liu Q Y, Wang W F, Tang J K. *Inorg. Chem.*, **2012**,**51**(4): 2381-2392

[14]Jiang Z Q, Jiang G Y, Hou D C, et al. *CrystEngComm*, **2013**,**15**(2):315-323

[15]Gao J Y, Xiong X H, Chen C J, et al. *Inorg. Chem. Commun.*, **2013**,**31**(5):5-12

[16]Xie W P, Wang N, Long Y, et al. *Inorg. Chem. Commun.*, **2014**,**40**(2):151-156

[17]Liu J X, Hu Y F, Zhu T. *CrystEngComm*, **2012**,**14**(20):6983 -6989

[18]LU Wen-Guan(卢文贯), LIU Hong-Wen(刘宏文). *Chinese J. Inorg. Chem.*(无机化学学报), **2010**,**26**(8):1450-1456